4-27-1999

The Influence of Surface Terminal Layer and Surface Defects on the Electronic Structure of CMR Perovskites: $La_{0.65}A_{0.35}MnO_3$ (A = Ca, Sr, Ba)

Jaewu Choi
University of Nebraska-Lincoln, jchoi@ece.eng.wayne.edu

Hani Dulli
University of Nebraska-Lincoln, hani.dulli@uconn.edu

Sy-Hwang Liou
University of Nebraska-Lincoln, sliou@unl.edu

Peter A. Dowben
University of Nebraska-Lincoln, pdowben@unl.edu

Marjorie Langell
University of Nebraska-Lincoln, mlangell1@unl.edu

Published in *physica status solidi (b)* **214** (1999), pp. 45–57.

Submitted January 27, 1999; revised April 27, 1999.

The Influence of Surface Terminal Layer and Surface Defects on the Electronic Structure of CMR Perovskites: $La_{0.65}A_{0.35}MnO_3$ (A = Ca, Sr, Ba)

Jaewu Choi [a], Hani Dulli [a], S.-H. Liou [a], P. A. Dowben [a], and M. A. Langell [b]

[a] Department of Physics and Astronomy and the Center for Materials Research and Analysis, Behlen Laboratory of Physics, University of Nebraska–Lincoln, Lincoln, Nebraska 68588-0111, USA
[b] Department of Chemistry, Hamilton Hall, University of Nebraska–Lincoln, Lincoln, Nebraska 68588-0304, USA
Corresponding author: P. A. Dowben, email: pdowben@unl.edu

Abstract: The electronic structure near to the Fermi level of the colossal magnetoresistance (CMR) perovskite manganite materials, $La_{0.65}A_{0.35}MnO_3$ (A = Ca, Sr, Ba), has been studied using both photoemission and inverse photoemission spectroscopy. The electronic structure for all three materials is very similar and consistent with an Mn–O terminal layer regardless of dopant. Small differences in the electronic structure among the materials are, however, observed. The observed band gap is not significant for $La_{0.65}Ca_{0.35}MnO_3$ and $La_{0.65}Ba_{0.35}MnO_3$ while there is a gap, about 1.5 eV, for $La_{0.65}Sr_{0.35}MnO_3$. There is a shift to higher binding energies of the extensively hybridized Mn–O Δ_5(e) bands for the surface (the surface on the Mn–O plane with C_{4v} symmetry) and t_{2g} bands for the bulk in the valence band spectra with increasing atomic number or atomic radius of dopants, approximately to 5.8, 6.8, and 7.8 eV for $La_{0.65}Ca_{0.35}MnO_3$, $La_{0.65}Sr_{0.35}MnO_3$, and $La_{0.65}Ba_{0.35}MnO_3$, respectively. The O–Mn–O terminal layer in these materials seems to be much more defect free than is the case for $La_{0.9}Ca_{0.1}MnO_3$, where the Ca–O terminal layer appears to be rich in defects.

1. Introduction

The colossal magnetoresistance (CMR) perovskite transition metal oxides, $La_{0.65}A_{0.35}MnO_3$ (A = Ca, Sr, Ba) [1–13] have been subject of theoretical [1, 14–21] and experimental [19–28] studies of the electronic structure. This series of transition metal oxides shows colossal magnetoresistance effects with different critical temperatures: ≈ 255 K for $La_{0.65}Ca_{0.35}MnO_3$, ≈ 350 K for $La_{0.65}Sr_{0.35}MnO_3$, and ≈ 325 K for $La_{0.65}Ba_{0.35}MnO_3$.

The termination layer of the perovskite manganese oxides, $La_{1-x}A_xMnO_3$ (A = Ca, Sr, Ba; x = 0.1, 0.35) has been studied using angle resolved X-ray photoemission spectroscopy [29–31], ion scattering spectroscopy [32, 33] and angle-resolved photoemission [19, 20, 26, 34]. The termination layer of $La_{0.9}Ca_{0.1}MnO_3$ is La–Ca–O layer [29, 30] but the termination layer of $La_{1-x}A_xMnO_3$, with x = 0.35, has been consistently determined to be an Mn–O [19, 20, 26, 32–34]. Differences in terminal layer with dopant concentration are interesting in view of the results

from studies of the electronic structure of $La_{0.65}A_{0.35}MnO_3$ (A = Ca, Sr, Ba) using surface sensitive spectroscopies, photoemission and inverse photoemission spectroscopy more sensitive to the O–Mn–O terminal layer than to the dopant and the dopant-containing A–O layers of the manganite perovskite.

Unfortunately, because the surface free energy is expected to be different from the bulk, surface segregation is expected. Surface segregation in ionic solids must be considered because of the existence of the space charge layer in the near surface region, providing a strong chemical potential. The bonding character of these transition metal oxides, $La_{1-x}A_xMnO_3$ (A = Ca, Sr, Ba), is mainly ionic. The surface segregation has been observed in many oxide alloys, including the surface segregation of calcium [35–37]. Surface segregation of calcium and strontium has now been observed in $La_{1-x}Ca_xMnO_3$ $La_{1-x}Ca_xMnO_3$ [29–30, 38] and $La_{1-x}Sr_xMnO_3$ [31, 39], respectively, prepared by several different techniques. With substantial segregation, the surface layer is compositionally a different material from the bulk.

The question arises as to whether, in the absence of careful surface compositional measurements, core level photoemission and the valence band electron spectroscopies are a good "fingerprint" of the different possible surface phases. This paper explores this issue.

2. Sample Preparation and Experimental Details

The crystalline samples were grown on (100) $LaAlO_3$ substrates by rf sputtering in a 5:1 argon/oxygen atmosphere (2:1 in the case of $La_{0.65}Sr_{0.35}MnO_3$) at 20 mTorr with the substrate maintained at a temperature of 700 °C. The films of $La_{0.65}Ca_{0.35}MnO_3$ and $La_{0.65}Ba_{0.35}MnO_3$ were annealed subsequently at 900 °C [26, 29, 30] and the films of $La_{0.65}Sr_{0.35}MnO_3$ were annealed at 900 °C in an oxygen atmosphere maintained at a pressure of 2 atm for 10 h. The bulk chemical composition of the films was determined from energy dispersive analysis of X-ray emission spectroscopy (XES or EDAX) and found to be similar to the targets with the final compositions $La_{0.65}Sr_{0.35}MnO_3$. The crystallinity and orientation was established by X-ray diffraction. The samples were further characterized by the temperature dependence of magnetoresistance. Sample surfaces were cleaned in ultra high vacuum by repeated annealing and exposure to low-energy electrons to stimulate the desorption of contaminants as described elsewhere [26].

The valence band spectra were taken using photoemission spectroscopy with He I (21.2 eV) and He II (40.8 eV) line discharge lamp light sources and a hemispherical electron energy analyzer. Spectra were taken with the photoelectrons collected at normal emission. The overall resolution of the photoemission spectra is 50 meV. The conduction band spectra were taken using inverse photoemission spectroscopy with a combination of a modified Zipf electron gun and a I_2 filled Geiger-Müller detector with CaF_2 window and the overall resolution is 450 meV in the same chamber (and therefore on the same surfaces). The inverse photoemission spectra were taken with normal incidence of electrons ($k_{||} = 0$). Surfaces of these films were prepared by annealing at 760 K for 2 h before taking data [26, 29, 30], and were characterized with core level photoemission.

X-ray photoemission spectroscopy was undertaken with the Mg-K_α line (1253.6 eV) from a PHI Model 04-548 Dual Anode X-ray source. Energy distribution curves of the elemental core levels were acquired with a large hemispherical electron energy analyzer (PHI Model 10-360 Precision Energy Analyzer). The core level spectra were measured at two different pass ener-

gies: 11.75 and 23.5 eV. The results were independent of pass energy, and therefore resolution. The Fermi level was established from tantalum in electrical contact with the sample. The binding energies of core levels are reported with respect to this Fermi level.

3. The Defects and Composition of the Surface

Core level photoemission data are shown for $La_{0.9}Ca_{0.1}MnO_3$, $La_{0.65}Ca_{0.35}MnO_3$ and $La_{0.65}Sr_{0.35}MnO_3$ in Figures 1 & 2. The differences in the termination layer appear to have only a small influence on the core level binding energies, as seen in Figs. 1 and 2. Both the core level binding energies and peak shapes are similar to those reported previously by Taguchi and Shimada [40] for $La_{1-x}Ca_xMnO_{2.97}$ and Saitoh et al. [21] for $La_{1-x}Sr_xMnO_3$. The core level data, nonetheless, generally suggest that the O–Mn–O terminal surfaces have fewer defects than is the case for the surface terminated in Ca–O, as described below.

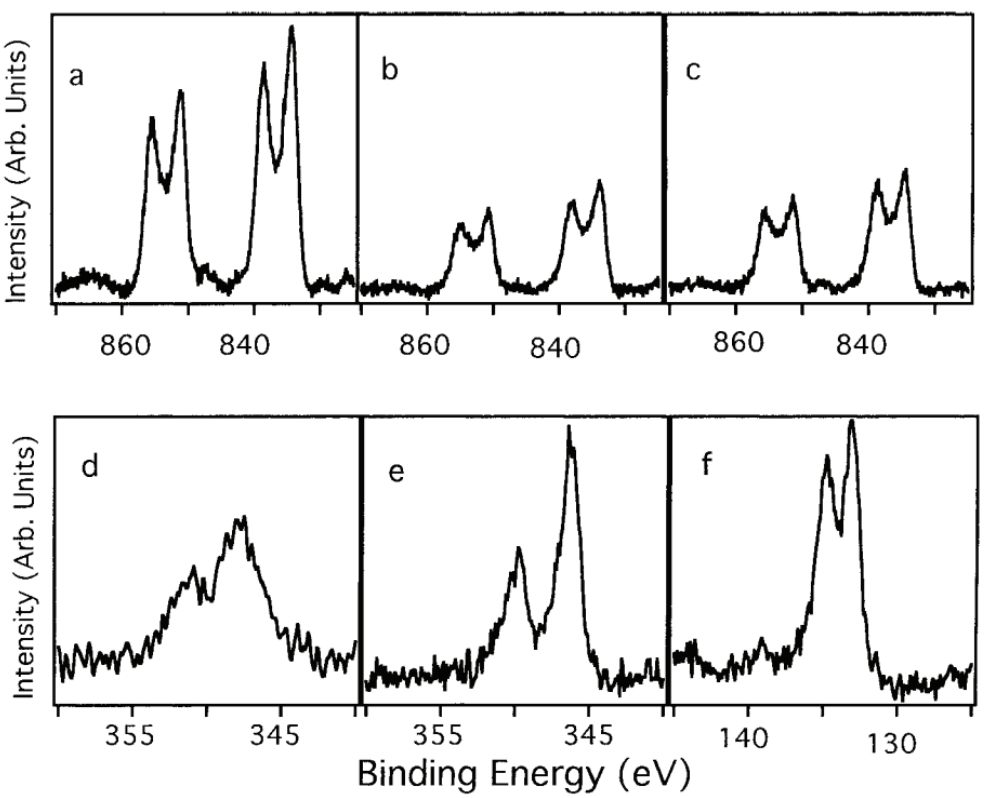

Figure 1. The La 3d core level spectra for a) La0.9Ca0.1MnO3, b) $La_{0.65}Ca_{0.35}MnO_3$ and c) $La_{0.65}Sr_{0.35}MnO_3$; the Ca 2p core level spectra for d) La0.9Ca0.1MnO3 and e) $La_{0.65}Ca_{0.35}MnO_3$; and f) the Sr 3d core level data for $La_{0.65}Sr_{0.35}MnO_3$. All data were taken at normal emission using Mg-Ka radiation (1253.6 eV) at an incidence angle of 60°

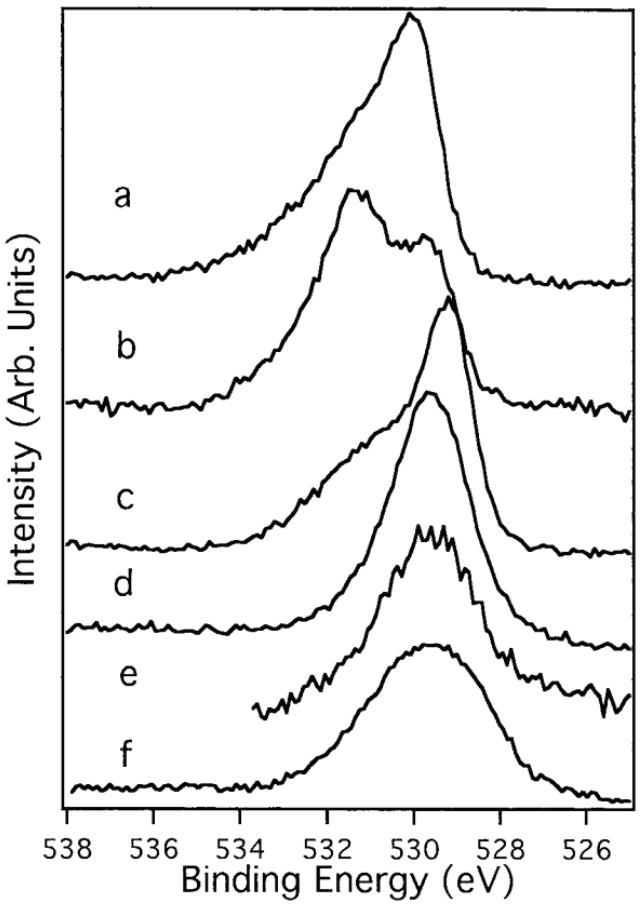

Figure 2. Comparison of the oxygen 1s core level spectra for
a) $La_{0.65}Sr_{0.35}MnO_3$,
b) $La_{0.9}Ca_{0.1}MnO_3$,
c) $La_{0.65}Ca_{0.35}MnO_3$,
d) Mn_2O_3,
e) Mn_3O_4, and
f) MnO.

It is now established [29, 30] that the surface of $La_{0.9}Ca_{0.1}MnO_3$ is dominated by huge amounts of Ca segregation and the Ca–O termination, unlike the majority O–Mn–O termination for $La_{0.65}Ca_{0.35}MnO_3$. The Ca $2p_{3/2}$ core level, at about 347.7 eV, for $La_{0.9}Ca_{0.1}MnO_3$ is both broader and at greater binding energy than for $La_{0.65}Ca_{0.35}MnO_3$, with a binding energy of nominally 346.3 eV, as seen in Figures 1d and e, respectively. In $CaMnO_{3-\delta}$ [41], as well as $La_{1-x}Ca_xMnO_{2.97}$ [40], a high binding energy satellite in the Ca core level spectrum has been identified separated by 1.1 eV or more to the main peak of the Ca $2p_{3/2}$ core level. This satellite binding energy increases with increasing calcium concentration and is believed to be strongly influenced by the oxygen content in the perovskite manganate [41].

The oxygen core level data also suggest the presence of defects in the Ca–O terminal layer of $La_{0.9}Ca_{0.1}MnO_3$. As shown in Figures 2 & 3, the oxygen 1s core level of the perovskite manganese oxides, $La_{1-x}A_xMnO_3$ (x = 0.1, 0.35; A = Ca, Sr), exhibits two dominant peaks, similar to those observed with high-T_c superconductors [42] and to epitaxial spinel oxides on rocksalt oxides [43, 44]. The binary manganese oxides show just one dominant O 1s peak, characteristic of the lattice O^{2-} and comparable to the lower binding energy peak of the perovskite materials. Thus the lower binding energy O 1s state corresponds to well ordered lattice oxygen. The higher binding energy O 1s peak found at 531.3 eV, in the perovskites, is related to either a different surface oxide or to oxygen associated with defects in the perovskite structure. The exact

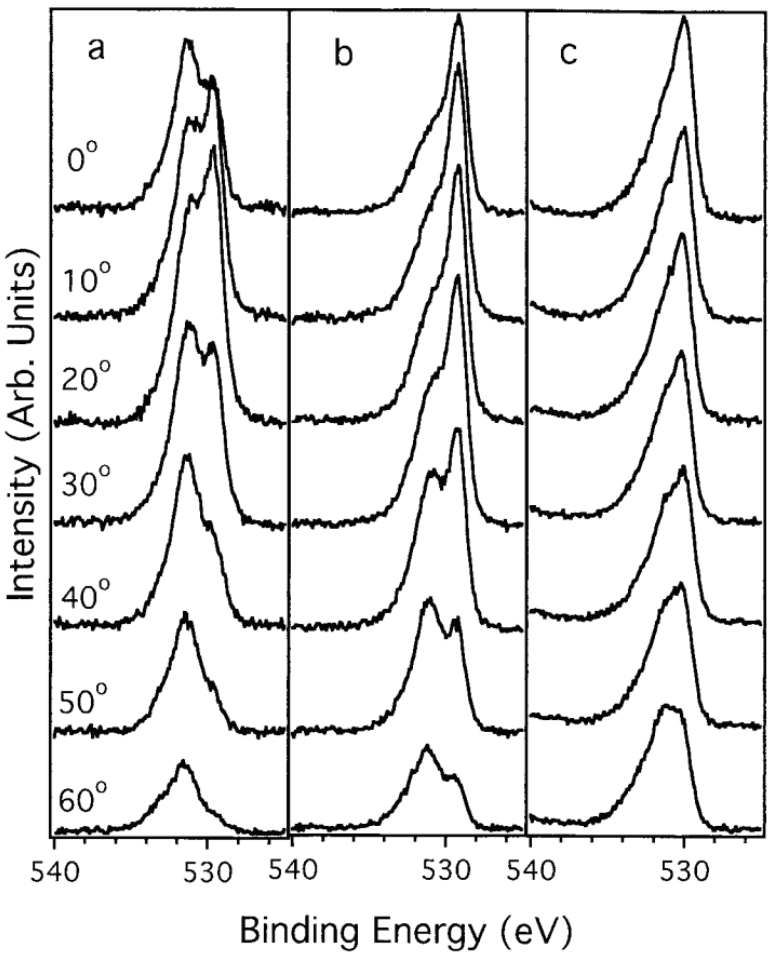

Figure 3. Oxygen 1s core level as a function of emission angle, with respect to the surface normal, for
a) $La_{0.9}Ca_{0.1}MnO_3$,
b) $La_{0.65}Ca_{0.35}MnO_3$, and
c) $La_{0.65}Sr_{0.35}MnO_3$

nature of the oxygen species giving rise to this 531.3 eV feature has not yet been determined. It has been proposed, however, that this 531.3 eV O 1s core level feature is associated with lattice defects in the oxide arising from metal vacancies and/or interstitials adjacent to the oxygen [42 to 44].

When the near surface distribution of the two different O 1s species was probed by changing the XPS emission angle (Figure 3), the higher binding energy species is seen to arise mainly from the outermost surface layers since it increases in intensity with larger emission angles. This is most clear for the $La_{1-x}Ca_xMnO_3$ (x = 0.1, 0.35) perovskites, but the effect is most dramatic for the lower bulk calcium concentration (x = 0.1). While the surface of $La_{0.9}Ca_{0.1}MnO_3$ is dominated by calcium segregation [29, 30], the surface cannot be considered to be completely "CaO-like." The Ca^{2+} species in the surface segregated layer is comparable, in binding energy, to that of calcium in CaO, the O 1s binding energy in CaO is found to be 530.2 [45, 46]. This is far too low relative to the observed values for the high binding energy feature observed here (531.3 eV).

CaO will not easily form an epitaxial layer on the top of the $La_{1-x}A_xMnO_3$ perovskite because of the substantial mismatch in lattice spacings. While both the rocksalt CaO and the perovskite

$La_{1-x}A_xMnO_3$ are cubic with (100) two dimensional surface geometries that are similar, the unit cell dimensions are very different with a = 4.799 Å for CaO [47] as opposed to (3.72 to 3.89) Å for $La_{1-x}Ca_xMnO_3$ [48]. Calcium does form a tetragonally distorted peroxide compound with the stoichiometry CaO_2 that has a square lattice plane with $a = b$ = 3.54 Å [48]. It is tempting to associate the oxygen species giving rise to the 531.3 eV binding energy O 1s XPS feature as oxygen in a "CaO-like" surface segregated phase, but the link cannot be made in a completely compelling fashion, as yet.

The $La_{0.9}Ca_{0.1}MnO_3$(100) surface terminates in the "Ca(La)–O" plane, with a significant excess of calcium [29, 30] and oxygen and with poor overall order, as is evident in the poor quality of the LEED [30] and the increased complexity of the XPS. The Mn 2p spectra from the sample indicate that the disorder is not limited to the Ca(La)–O surface layer alone. The full widths at half maximum (FWHM) of the Mn 2p core level spectra are shown as a function of the emission angle for $La_{0.9}Ca_{0.1}MnO_3$ (open circles), $La_{0.65}Ca_{0.35}MnO_3$ (filled circles) and $La_{0.65}Sr_{0.35}MnO_3$ (squares) in Figure 4. For the $La_{0.9}Ca_{0.1}MnO_3$ Mn $2p_{3/2}$ spectrum, the FWHM value increases with increasing emission angle, which increases the surface sensitivity. By comparison, the $La_{0.65}A_{0.35}MnO_3$ (A = Ca, Sr) manganese 2p spectrum remains relatively constant in peak shape regardless of the emission angle (depth sampled). Uhlenbrock *et al.* [49] have used the FWHM emission angle dependence on the Ni 2p and O 1s core level spectra, in a similar way, to deduce the presence of surface defects on NiO. Although the materials discussed here are different from the simple NiO structure, the implication that a wide range of Mn-related species is found in the Ca-segregated surface is quite striking and equally valid.

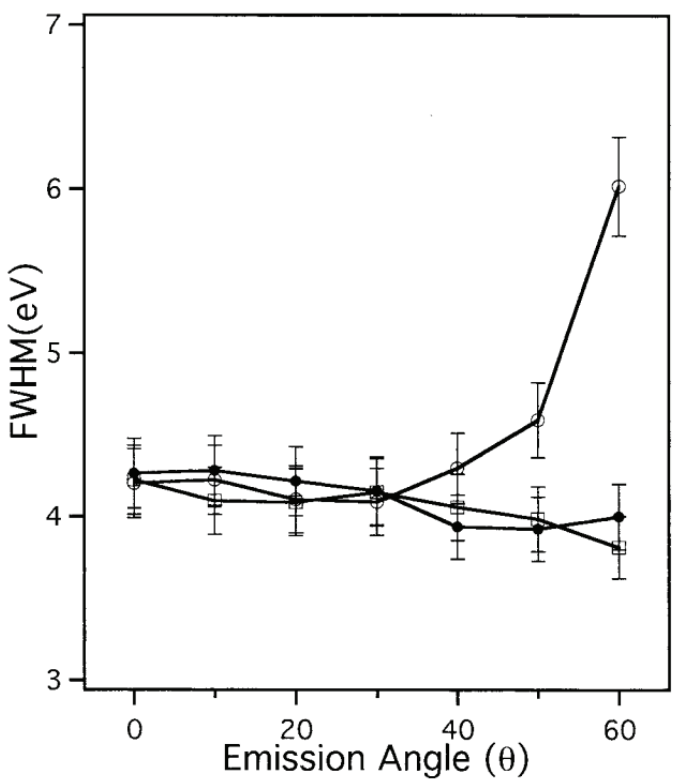

Figure 4. The full width at half maximum (FWHM) of the Mn $2p_{3/2}$ core level for $La_{0.9}Ca_{0.1}MnO_3$ (○), $La_{0.65}Ca_{0.35}MnO_3$ (●), and $La_{0.65}Sr_{0.35}MnO_3$ (□).

For the $La_{0.65}A_{0.35}MnO_3$ (A = Ca, Sr) materials, the surface is seen to terminate in O–Mn–O [26, 29–34] and a more homogeneous surface with far fewer surface defects is apparent. The Mn $2p_{3/2}$ core level binding energies (shown in Figure 5) of 642.5 eV (A = Sr) and 641.8 eV (A = Ca) are slightly greater than those observed for Mn_2O_3 (641.1 eV), Mn_3O_4 (641.6 eV), and MnO (640.6 eV) and consistent with those binding energies previously measured by Taguchi and Shimada [40] for $La_{1-x}Ca_xMnO_{2.97}$ and Saitoh *et al.* [21] for $La_{1-x}Sr_xMnO_3$. Taguchi and Shimada [40] propose that these binding energies are consistent with a combination of Mn^{3+} and Mn^{4+} states as represented by $LaMn^{3+}O_3$ (642.0 eV) and $Mn^{4+}O_2$ (642.4 eV) [50–52]. This assignment is consistent with the fact that Sr segregation [31] is far more pronounced than Ca segregation to the subsurface layer of $La_{0.65}A_{0.35}MnO_3$ (A = Ca, Sr). Thus the surface of $La_{0.65}A_{0.35}MnO_3$ (A = Sr) should be dominated by more Mn^{4+} species than the surface of $La_{0.65}A_{0.35}MnO_3$ (A = Ca) and the unresolved Mn^{4+}/Mn^{3+} 2p spectra should shift to higher binding energy. The independence of the FWHM of the $La_{0.65}A_{0.35}MnO_3$ (A = Ca, Sr) manganese core level with emission angle suggests little evidence of a surface Mn species that differs substantially from the bulk (Figure 4).

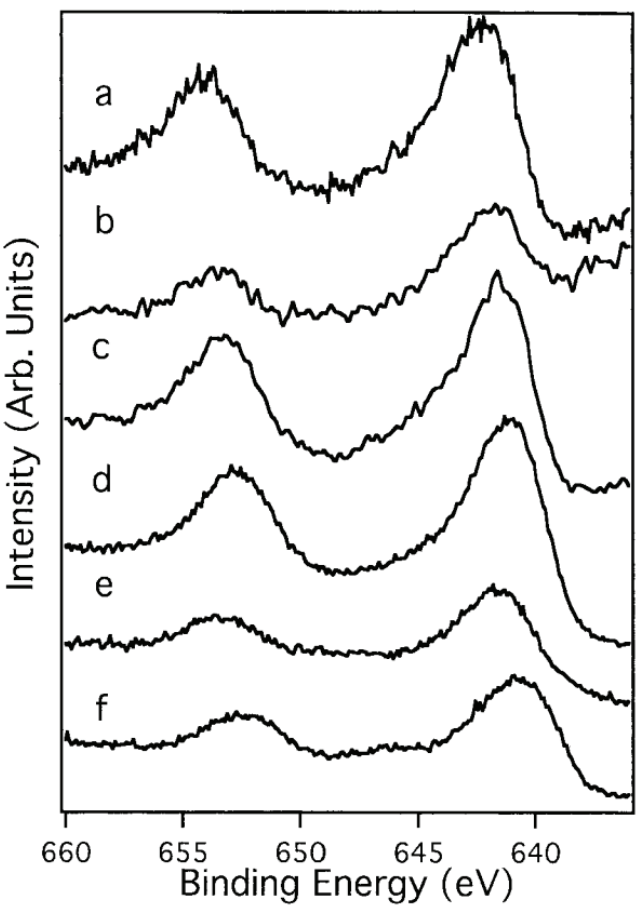

Figure 5. Comparison of the Mn $2p_{3/2}$ core level for
a) $La_{0.65}Sr_{0.35}MnO_3$,
b) $La_{0.9}Ca_{0.1}MnO_3$,
c) $La_{0.65}Ca_{0.35}MnO_3$,
d) Mn_2O_3,
e) Mn_3O_4, and
f) MnO

In either case, because of either massive Ca segregation [29, 30] or the O–Mn–O termination [26, 29–34], the La 3d core level, seen in Figures 1a–c, is representative of a more bulk-like species. Figure 1 shows the La 3d core level spectra measured at normal emission for $La_{0.9}Ca_{0.1}MnO_3$, $La_{0.65}Ca_{0.35}MnO_3$ and $La_{0.65}Sr_{0.35}MnO_3$, respectively. Each spin-orbit component shows the two distinct features due to the main peak and shake up satellites commonly observed for La^{3+} oxides [53–56] and these perovskites [40].

4. The Contribution of the Terminal Layer to the Electronic Structure

The electronic valence and conduction band structure was studied at room temperature, as shown in Figure 6. The samples are in different bulk phases at this temperature due to the different critical temperatures so that at room temperature the bulk of $La_{0.65}Ca_{0.35}MnO_3$ is in the nonmetallic-paramagnetic phase, $La_{0.65}Sr_{0.35}MnO_3$ is in the metallic-ferromagnetic phase, and $La_{0.65}Ba_{0.35}MnO_3$ is in the metallic-ferromagnetic phase. The valence band spectra shown were taken using the He I (21.2 eV) line source for $La_{0.65}Ca_{0.35}MnO_3$ (Figure 6a, left) and $La_{0.65}Ba_{0.35}MnO_3$ (Figure 6c, left) and the He II (40.8 eV) line for $La_{0.65}Sr_{0.35}MnO_3$ (Figure 6b, left). As with studies undertaken with synchrotron light sources [26], we observe that the overall valence band width of the photoemission spectra for $La_{0.65}Sr_{0.35}MnO_3$ and for $La_{0.65}Ba_{0.35}MnO_3$ is larger than for $La_{0.65}Ca_{0.35}MnO_3$. This is consistent with the greater band dispersion and concomitant greater band widths with the "larger" dopants [26] Sr and Ba.

The electronic valence band structure of the manganese transition metal oxides, $La_{0.65}A_{0.35}MnO_3$ (A = Ca, Sr, Ba), is mostly dominated by the extensively hybridized Mn 3d–O 2p states [14–27]. The electronic valence band structure of $La_{0.65}Ca_{0.35}MnO_3$ was studied using photoemission and resonant photoemission spectroscopy [19] and the spectra were fitted with seven Gaussian peaks which have different origins. The resolved feature at 5.8 eV was considered to be a combination of extensively hybridized Mn $3d_{xz,yz}$–O $2p_{xy}$ states or Mn–O Δ_5 (e) bands for the O–Mn–O surface, with C_{4v} symmetry, and t_{2g} bands for the bulk in the valence band spectra.

Based on these band assignments of the valence band spectra, the corresponding extensively hybridized states are shifted to 6.8 eV for films of $La_{0.65}Sr_{0.35}MnO_3$ and to 7.8 eV for films of $La_{0.65}Ba_{0.35}MnO_3$. The shifts of the Mn 3d–O 2p hybridization states come from the strong influence of the overlap of the hole dopant orbital to the oxygen 2p orbital. With increasing atomic radius of the hole dopant from Ca to Ba, the overlap between the valence states of the dopant and the oxygen 2p states appears to increase. As expected, in the Hückel orbital overlap picture, the result of increased hybridization shifts the Mn 3d–O 2p states to higher binding energy with increasing atomic radius of the hole dopants. This is clearly seen in Figure 6.

The low binding energy valence band states in the 1 to 6 eV region of $La_{0.65}Sr_{0.35}MnO_3$ in Figure 6, originate from the Mn 3d derived levels [20] and have comparatively larger intensities than for $La_{0.65}Ca_{0.35}MnO_3$ (Figure 6a, left) and of the $La_{0.65}Ba_{0.35}MnO_3$ (Figure 6c, left). Furthermore, the intensity of $La_{0.65}Sr_{0.35}MnO_3$ at the Fermi level in the valence band spectra is almost negligible compared to the valence band spectra intensity at the Fermi level for both $La_{0.65}Ca_{0.35}MnO_3$ and $La_{0.65}Ba_{0.35}MnO_3$ (Figure 6). These differences may actually be due to the dopant since $La_{0.65}Ca_{0.35}MnO_3$ and $La_{0.65}Ba_{0.35}MnO_3$ exhibit much less Ca or Ba surface segregation [29–31] than is observed for $La_{0.65}Sr_{0.35}MnO_3$ [31]. Thus the near surface region of $La_{0.65}Sr_{0.35}MnO_3$ is nearly $SrMnO_3$ and/or Sr_2MnO_4, though this effect is larger in the subsurface layer than in the outermost layer itself [31].

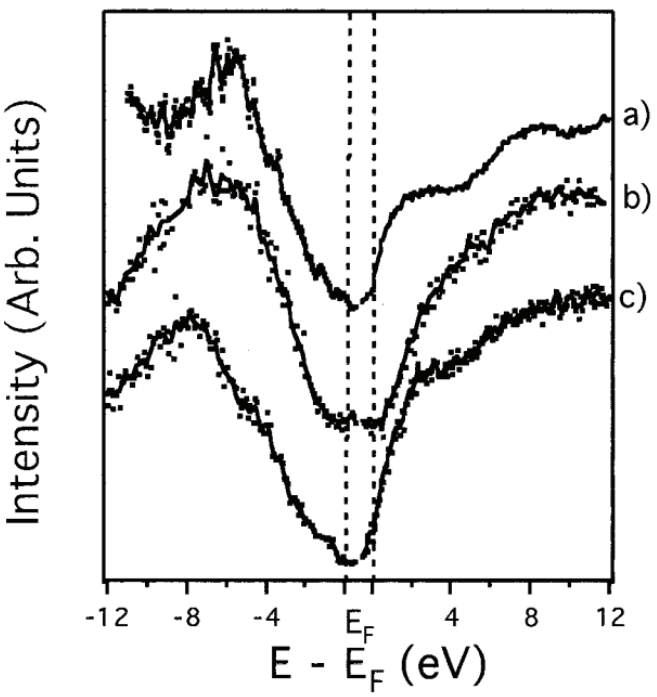

Figure 6. The electronic valence and conduction band structure of

a) $La_{0.65}Ca_{0.35}MnO_3$,
b) $La_{0.65}Sr_{0.35}MnO_3$, and
c) $La_{0.65}Ba_{0.35}MnO_3$.

The photoemission spectra for the valence band spectra (left) are taken at room temperature and at normal emission of photoelectrons using He I (for $La_{0.65}Ca_{0.35}MnO_3$ and $La_{0.65}Ba_{0.35}MnO_3$) and He II (for $La_{0.65}Sr_{0.35}MnO_3$) lines as light sources. The inverse photoemission spectra for the conduction band structure (right) are taken at room temperature and at normal incidence of electrons using an isochromatic mode (scan with incident electron kinetic energy of 5 to 19 eV, detected with a fixed photon energy of 9.8 eV).

The inverse photoemission spectra for the conduction band structure are shown at the right in Figure 6. There are two main features at ≈ 3 and 8 eV above the Fermi level. The feature at ≈ 3 eV above the Fermi level is generally considered to correspond to the nonbonding or antibonding-like states with Mn 3d–O 2p hybridized character [27]. The higher energy feature at 8 eV above the Fermi level corresponds to the La 4f states [27, 28]. The antibonding-like states of the Mn 3d–O 2p states are positioned at approximately 2 eV above the Fermi level for both $La_{0.65}Ca_{0.35}MnO_3$ and $La_{0.65}Ba_{0.35}MnO_3$ while the antibonding-like states of the Mn 3d–O 2p hybridization states for the $La_{0.65}Sr_{0.35}MnO_3$ are at about 4 eV above the Fermi level.

The features at 8 eV in the conduction band inverse photoemission spectra, corresponding to the La 4f states [27, 28], are clearly observed in the conduction band of $La_{0.65}Ca_{0.35}MnO_3$ while the La 4f states for $La_{0.65}Sr_{0.35}MnO_3$ are substantially broader and less apparent. The La 4f states for $La_{0.65}Ba_{0.35}MnO_3$ are barely distinguishable. The peak broadening of the valence and the La 4f states in the conduction band could be related to the metallic properties. Above the critical temperature, in the nonmetallic phase, the features are much sharper than below the critical temperature in the metallic phase for $La_{0.65}Ca_{0.35}MnO_3$ (Figure 7). In general, the similarity of the spectra in Figure 6 argues in favor of the model proposed, by Taguchi and Shimada [40] for $La_{1-x}Ca_xMnO_{2.97}$, that the bonding is generally covalent and not ionic for the more heavily doped species.

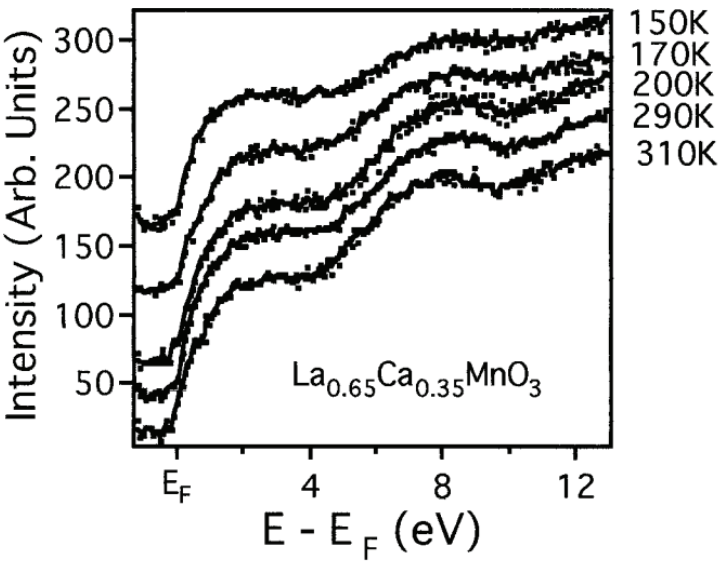

Figure 7. Temperature dependence of the conduction band electronic structure from inverse photoemission. The spectra were taken for electrons at normal incidence to the surface of $La_{0.65}Ca_{0.35}MnO_3$, *i.e.*, no electron wave vector parallel to the surface.

The unoccupied electronic structure of $La_{0.65}Ca_{0.35}MnO_3$ films was studied as a function of temperature as shown in Figure 7. The dominant change in the unoccupied electronic structure with increasing temperature is the increasing intensity of the La 4f state feature which is at 8 eV above the Fermi level. The density of states near to the Fermi level in the valence band was seen to decrease with increasing temperature [24, 26] in several different studies. Measurements have also been undertaken indicating a change in the screening parameter that accompanies the changes in the occupied density of states [24, 26]. This is known to affect the unoccupied state line shape [57]. Therefore, we postulate that the La 4f states could be an electron reservoir. Dynamic motions of the lattice can cause an increase in the spectral line widths, but such changes usually cause an increase in the measured feature widths with increasing temperature [58] and are therefore unlikely to be the origin of the changes observed here. All of the temperature dependent changes in electronic structure of $La_{0.65}Ca_{0.35}MnO_3$ reported here or previously [24, 26] affect the electronic density of states and the associated screening parameter near the Fermi level is small. Nonetheless, even for $La_{0.65}Ca_{0.35}MnO_3$ the temperature dependent changes in electronic structure appear to be greater than the effect of changing the dopant to another alkaline earth metal.

With significant surface segregation, the surface electronic structure is seen to vary substantially in photoemission and inverse photoemission, as will be discussed in detail elsewhere for $La_{0.65}Sr_{0.35}MnO_3$ [31], but then the surface is essentially a different material from the bulk. The more modest segregation observed for $La_{0.65}Ca_{0.35}MnO_3$ appears to have little influence on the core level spectra, as noted above, and very little influence over the valence and conduction band regions near the Fermi level.

A profound influence on the density of states near the Fermi level is a consequence of defects, as has already been noted [26]. This is consistent with the changes observed in the core level spectra noted above.

5. Summary

In summary, there is little significant dependence of the hole dopants (Ca, Sr, Ba) in the electronic structure of the colossal magnetoresistance (CMR) perovskite transition metal oxides, $La_{0.65}A_{0.35}MnO_3$ (A = Ca, Sr, Ba), when the surfaces are prepared in an identical fashion. Both surface states [26] and the identical terminal layer [26, 29] are seen to dominate both photoemission and inverse photoemission minimizing the influence of the dopant in electron spectroscopy. The changes due to doping appear to be more subtle. The larger physical size of the hole dopant creates stronger hybridization of the Mn 3d–O 2p levels and appears to induce a shift of the Mn 3d–O 2p states to the higher binding energy in photoemission with increased hybridization. The valence and conduction band spectra of the $La_{0.65}Sr_{0.35}MnO_3$ films have a small to negligible density of the states near Fermi level, unlike those observed for $La_{0.65}Ca_{0.35}MnO_3$ and $La_{0.65}Ba_{0.35}MnO_3$. We caution spectroscopists—before attributing changes in the electronic structure to dopant effects—to carefully eliminate differences in the surface structure, surface composition [29] and, as noted elsewhere [26, 31], temperature.

Surface segregation in the complex oxides is relatively common [29–31] and can affect the unoccupied La 4f state electronic structure substantially. This influence of the surface segregation and surface defects does appear to have some, albeit small, effect upon the core level binding energies, though, as we postulate here, the influence of defects appears to be much more pronounced, as the influence of defects on the photoemission and inverse photoemission is quite dramatic [26].

Acknowledgements: This work was supported by NSF through grants No. DMR-9802126 and CHE-9616690 and the Joint Center for Atom Technologies (JRCAT) through the Atomic Technology Partnership and the Center for Materials Research and Analysis (CMRA) at the University of Nebraska–Lincoln.

References

[1] M. Imada, A. Fujimori, and Y. Tokura, *Rev. Mod. Phys.* **70**, 1039 (1998).

[2] A.P. Ramirez, *J. Phys.: Condensed Matter* **9**, 8171 (1997).

[3] N. Sharma, A.K. Nigam, R. Pinto, N. Venkatarani, S. Prasod, G. Chandra, and S.P. Pai, *J. Magn. Magn. Mater.* **154**, 296 (1996).

[4] M.F. Hundley, J.J. Neumeier, R.H. Heffner, Q.X. Jia, X.D. Wu, and J.D. Thompson, *J. Appl. Phys.* **79**, 4535 (1996).

[5] K-i. Chahara, T. Ohno, M. Kasai, and Y. Kozono, *Appl. Phys. Lett.* **63**, 1990 (1993).

[6] N. Furukawa, *J. Phys. Soc. Jpn.* **64**, 3164 (1995).

[7] N. Furukawa, *J. Phys. Soc. Jpn.* **64**, 2754 (1995).

[8] Y. Tokura, A. Urushibara, Y. Morimoto, T. Arima, A. Asamitsu, G. Kido, and N. Furukawa, *J. Phys. Soc. Jpn.* **63**, 3931 (1994).

[9] Y. Tokura, Y. Tomioka, H. Huwahara, A. Asamitsu, Y. Moritomo, and M. Kasai, *J. Appl. Phys.* **79**, 5288 (1996).

[10] S.E. Lofland, S.M. Bhagat, H.L. Ju, G. C. Xiong, T. Venkatesan, R.L. Greene, and S. Tyagi, *J. Appl. Phys.* **79**, 5166 (1996).

[11] R. von Helmolt, J. Wecker, B. Holzapfel, L. Schultz, and K. Samwer, *Phys. Rev. Lett.* **71**, 2331 (1993).

[12] P. Schiffer, A.P. Ramirez, W. Bao, and S.-W. Cheong, *Phys. Rev. Lett.* **75**, 3336 (1995).

[13] Z. Trajanovic, C. Kwon, M.C. Robson, K.-C. Kim, M. Rajeswari, R. Ramesh, T. Venkatesan, S.E. Lofland, S.M. Bhagat, and D. Fork, *Appl. Phys. Lett.* **69**, 1005 (1996).

[14] J.M.D. Coey, M. Viret, L. Ranno, and K. Ounadjela, *Phys. Rev. Lett.* **75**, 3910 (1995).

[15] D.D. Sarma and S.R. Barman, in: *Spectroscopy of Mott Insulators and Correlated Metals,* Eds. A. Fujimori and Y. Tokura, Springer Series in Solid-State Sciences, Vol. 119, SpringerVerlag, Berlin/Heidelberg/New York 1995 (p. 126).

[16] S. Satpathy, Z.S. Popovic, and F.R. Vukajlovic, *Phys. Rev. Lett.* **76**, 960 (1996).

[17] A.J. Millis, P.B. Littlewood, and B.I. Shraiman, *Phys. Rev. Lett.* **74**, 5144 (1995).

[18] J. Zaanen, G.A. Sawatzky, and J.W. Allen, *Phys. Rev. Lett.* **55**, 418 (1985).

[19] Jiandi Zhang, D.N. McIlroy, P.A. Dowben, S.-H. Liou, R.F. Sabirianov, and S.S. Jaswal, *Solid State Commun.* **97**, 39 (1996).

[20] C. Waldfried, D.N. McIlroy, S.-H Liou, R. Sabiryanov, S.S. Jaswal, and P.A. Dowben, *J. Phys.: Condensed Matter* **9**, 1031 (1997).

[21] T. Saitoh *et al., Phys. Rev. B* **51**, 13942 (1995).

[22] J.-H. Park, C.T. Chen, S.-W. Cheong, W. Bao, G. Meigs, V. Chakarian, and Y.U. Idzerda, *J. Appl. Phys.* **79**, 4558 (1996).

[23] J.-H. Park, E. Vescovo, H.J. Kim, C. Kwon, R. Ramesh, and T. Venkatesan, *Nature* **392**, 794 (1998).

[24] D.N. McIlroy, J. Zhang, S.-H. Liou, and P.A. Dowben, *Phys. Lett. A* **207**, 367 (1995); J.-H. Park, C.T. Chen, S.-W. Cheong, W. Bao, G. Meigs, V. Chakarian, and Y.U. Idzerda, *Phys. Rev. Lett.* **76**, 4215 (1996).

[25] M. Abbate et al., *Phys. Rev. B* **46**, 4511 (1992).

[26] D.N. McIlroy, C. Waldfried, Jiandi Zhang, Jaewu Choi, F. Foong, S.-H. Liou, and P.A. Dowben, *Phys. Rev. B* **54**, 17438 (1996).

[27] A. Chainani, M. Mathew, and D.D. Sarma, *Phys. Rev. B* **47**, 15397 (1993).

[28] S. Suga, S. Imada, T. Muro, T. Fukawa, T. Shishidou, Y. Yokura, Y. Moritomo, and T. Miyahara, *J. Electron Spectroscopy Related Phenomena* **78**, 283 (1996).

[29] Jaewu Choi, C. Waldfried, S.-H. Liou, and P.A. Dowben, *J. Vacuum Sci. Technol. A* **16**, 2950 (1998).

[30] Jaewu Choi, Jiandi Zhang, S.-H. Liou, P.A. Dowben, and E.W. Plummer, *Phys. Rev. B* **59**, 13453 (1999).

[31] Hani Dulli, P. A. Dowben, Jaewu Choi, S.-H. Liou, and E.W. Plummer, submitted to *Science*.

[32] M. Yoshimoto, H. Maruta, T. Ohnishi, K. Sasaki, and H. Koinuma, *Appl. Phys. Lett.* **73**, 187 (1998).

[33] M. Izumi, Y. Konishi, T. Nishihara, S. Hayashi, M. Shinohara, M. Kawasaki, and Y. Tokura, *Appl. Phys. Lett.* **73**, 2497 (1998).

[34] A.A. Zakharov, H. NyleÂn, M. Quavford, I. Lindau, M. Leandersson, M.B. Tsetlin, and M.N. Mikheeva, *Phys. Rev. B* **56**, 9030 (1997).

[35] E.A. Colbourn, W.C. Mackrodt, and P.W. Tasker, *J. Mater. Sci.* **18**, 1917 (1983).

[36] W.C. Mackrod and P.W. Tasker, *J. Amer. Ceram. Soc.* **72**, 1576 (1989).

[37] R.C. McCune and P. Wynblant, *J. Amer. Ceram. Soc.* **66**, 111 (1983).

[38] Wei Zhang, Xiaoru Wang, and I. Boyd, *Appl. Phys. Lett.* **73**, 2745 (1998).

[39] L.-C. Dufour, G.L. Bertrand, G. Caboche, P. Decorse, A. El Anssari, A. Poirson, and M. Vareille, *Solid State Ionics* **101**/**103**, 661 (1997).

[40] H. Taguchi and M. Shimada, *J. Solid State Chem.* **67**, 37 (1987).

[41] H. Taguchi and M. Shimada, *phys. stat. sol. (b)* **131**, K59 (1985).

[42] P. Steiner, R. Courths, V. Kinsinger, I. Sander, B. Siegwart, S. HuÈfner, and C. Politis, *Appl. Phys. A* **44**, 75 (1987).

[43] G.A. Carson, M.H. Nassir, and M.A. Langell, *J. Vacuum Sci. Technol.* **14**, 1637 (1996).

[44] M. Oku and Y. Sato, *Appl. Surf. Sci.* **55**, 37 (1992).

[45] G. Chiarello, A. Lumachi, and F. Parmagian, *J. Electron Spectroscopy Related Phenomena* **50**, 229 (1990).

[46] D. Berruto, L. Barco, G. Balleri, and A.W. Searcy, *J. Amer. Ceram. Soc.* **64**, 74 (1981).

[47] G.V. Samsanov (Ed.), *The Oxide Handbook,* IFI/Plenum Press, New York 1973.

[48] P. Dai, J. Zhang, H.A. Mook, F. Foong, S.-H. Liou, P.A. Dowben, and E.W. Plummer, *Solid State Commun.* **100**, 865 (1996).

[49] S. Uhlenbrock, C. Scharfschwerdt, M. Neumann, G. Illing, and H.-J. Freund, *J. Phys.: Condensed Matter* **4**, 7973 (1992).

[50] D.J. Lam, B.W. Veal, and D.E. Ellis, *Phys. Rev. B* **22**, 5730 (1972).

[51] J.C. Carver, G.K. Scheritzer, and T.A. Carlson, *J. Chem. Phys.* **57**, 973 (1972).

[52] S.P. Kowalczyk, L. Ley, F.R. McFeely, and D.A. Shirley, *Phys. Rev. B* **11**, 1721 (1975).

[53] A.E. Bocquet, T. Mizokawa, T. Saitoh, H. Namatame, and A. Fujimori, *Phys. Rev. B* **46**, 3771 (1992).

[54] H.R. Moser, B. Delley, W.D. Schneider, and Y. Baer, *Phys. Rev. B* **29**, 2947 (1984).

[55] G. Crecelius, G.K. Wertheim, and D.N. Buchanan, *Phys. Rev. B* **18**, 6519 (1978).

[56] J.C. Fuggle, O. Gunnarsson, G.A. Sawatzky, and K. Schonhammer, *Phys. Rev. B* **37**, 1103 (1988).

[57] C.M. Teodorescu, D. Gravel, Jaewu Choi, D. Pugmire, P. A. Dowben, and E. Rühl, *Europ. J. Chem.*, submitted.

[58] C. Waldfried, D.N. McIlroy, J. Zhang, P.A. Dowben, G.A. Katrich, and E.W. Plummer, *Surface Sci.* **363**, 296(1996); Jaewu Choi, P.A. Dowben, S. Pebley, A. Bune, S. Ducharme, V.M. Fridkin, S.P. Palto, and N. Petukhova, *Phys. Rev. Lett.* **80**, 1328 (1998).